

Perturbation Size and Harmonic Limitations in Affine Approximation for Time Invariant Periodicity Preservation Systems

Josh Martin, *Student Member, IEEE*, Charles Baylis, *Member, IEEE* and Robert J. Marks II, *Fellow, IEEE*, and Matthew Moldovan, *Student Member, IEEE*

Abstract— Affine approximation is a technique used to model time-invariant periodicity preservation (TIPP) systems, which represent a broad class of wireless system nonlinear components. This approach approximates the harmonic transfer characteristics of a nonlinear system and, as a consequence, is expected to be very useful in both waveform design and circuit optimization. While this approach is useful, there are limitations of this approximation based on the strength of the nonlinearity, the size of the perturbation imposed on the large-signal operating condition, and the number of harmonics used to approximate the signal. This paper examines some sample TIPP nonlinearities and show that the affine approximation accuracy often degrades for increasing perturbation size and when a reduced number of harmonics is used to approximate system results for waveforms containing significant harmonic content.

I. INTRODUCTION

Modeling time-invariant periodicity preservation (TIPP) systems using nonlinear network parameters can allow prediction of nonlinear system behavior under certain large-signal excitation conditions [1]. Because this approach directly predicts the transfer between harmonics, it is useful for waveform design and optimization. Successfully modeling the harmonic transfer characteristics of a system will allow optimization of both circuit and waveform to meet spectral requirements, in concert with efforts and descriptions provided in [2, 3, 4]. Similar groundbreaking nonlinear system harmonic coupling characterizations [5, 6, 7, 8, 9] such as VIOMAP [10], S-functions [11, 12, 13, 14], polyharmonic distortion (PHD) models [15, 16, 17, 18, 19] and X-parameters [20, 16, 21, 22, 23, 24, 25, 26, 27, 12, 28, 29, 30] have been offered as approaches to the “black-box” modeling of nonlinear devices. These approaches differ from more traditional nonlinear models such as Volterra [31] and Hermite [32] characterizations in that they use straightforward harmonic measurements that can be performed in the laboratory. [33]. Modeling nonlinear devices as time-invariant periodicity preservation (TIPP) systems can result in reasonable approximation of the system’s harmonic transfer characteristics under large-signal excitation. The theory of TIPP systems has been presented in detail by our group in [1]. Finding the TIPP parameters of a device is an approach to black-box nonlinear modeling that circumvents (in some cases, with limited accuracy) the significant measurement time and modeling effort required to extract a nonlinear model for

the device. A TIPP system operates on the input Fourier series coefficients \vec{i} and to produce the output Fourier series coefficients \vec{v} . This relationship can be interpreted as a nonlinear extension of Ohm’s Law [1], which reduces to a linear relationship for the linear time-invariant (LTI) case. Analysis of the TIPP harmonic mixing requires that the system be represented in the frequency domain. The TIPP system can be represented by the operator \mathcal{Z} such that

$$\vec{v} = \mathcal{Z}\vec{i} \quad (1)$$

A property of TIPP systems is that the output signal must possess the same fundamental period as the input. Affine modeling of a TIPP system attempts to define a region centered on an original large-signal “operating point” for which other nearby points can be approximated. Superimposing a small perturbation with Fourier coefficient vector $\Delta\vec{i}$ atop the large signal with Fourier coefficient vector \vec{i} produces [1]

$$\vec{v}_\Delta := \mathcal{Z}\{\vec{i} + \Delta\vec{i}\}. \quad (2)$$

\vec{v}_Δ is the vector of the output Fourier series coefficients given by this affine approximation. For sufficiently smooth perturbations, TIPP system’s can be approximated by [1]

$$\vec{v}_\Delta \simeq \mathcal{Z}\vec{i} + \nabla\mathcal{Z}_{\vec{v}}(\vec{i})\Delta\vec{i} = \vec{v} + \Delta\vec{v} \quad (3)$$

where $\Delta\vec{v} = \nabla\mathcal{Z}_{\vec{v}}(\vec{i})\Delta\vec{i}$ and $\nabla\mathcal{Z}_{\vec{v}}(\vec{i})$ is the Jacobian of the TIPP system about the operating point. The Jacobian is a matrix whose elements are

$$[\nabla\mathcal{Z}_{\vec{v}}(\vec{i})]_{nm} := \left[\frac{\partial v_n}{\partial i_m} \right]_{\vec{i}} \quad (4)$$

The accuracy of the affine approximation behavior depends significantly on (1) the size of the perturbation and (2) the number of harmonics considered in the approximation. For more severe system nonlinearities and for waveforms requiring a large number of harmonics for complete description, the affine approximation accuracy can be significantly reduced. This paper contains a number of

simulations of errors resulting from the approximation for various TIPP systems and perturbations.

II. TIPP SIMULATIONS

A simple operating point and perturbation will be chosen to show the effects of perturbation size and nonlinearity strength for low harmonic input levels. The relative error of each approximation is measured using percent RMS Error:

$$\% \text{ RMS Error} = \sqrt{\frac{\sum_{i=1}^n (\text{Actual} - \text{Approx})^2}{\sum_{i=1}^n (\text{Actual})^2}} \times 100 \quad (5)$$

We consider the case where the temporal output is a nonlinear function of the input, i.e.

$$v(t) = g(i(t)). \quad (6)$$

When $i(t)$ is periodic with period T then, for any function $g(i(t))$ will be periodic with the same period. The Fourier coefficients are extracted from these periodic signals and they are used to establish the TIPP relationship in (1) about some operating point. Some useful nonlinearities are shown in Fig. 1. Fig. 1(a) shows a linear system, given by

$$g(i) = i. \quad (7)$$

Fig. 1(b) shows an operation of full-wave rectification, given by

$$g(i) = |i|. \quad (8)$$

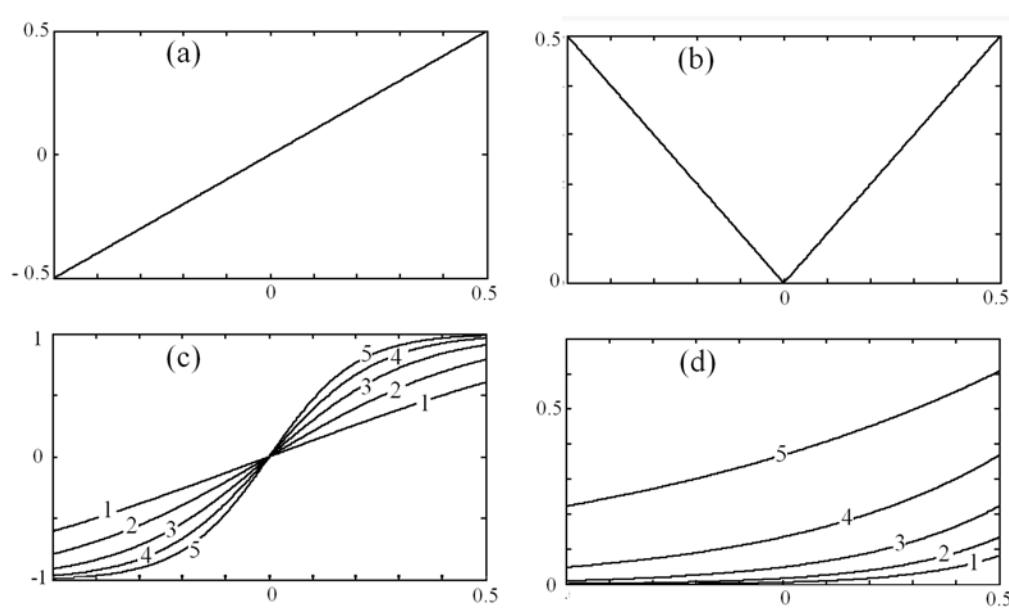


Fig. 1. Nonlinearities, $g(i)$ for $-0.5 \leq i \leq 0.5$ (a) Linear, $g(i) = i$. (b) Full wave rectifier $g(i) = |i|$. (c) Sigmoid, $g(i) = \tanh(\alpha i)/\tanh(\alpha)$ for $\alpha = 1, 2, 3, 4, 5$. (d) Exponential $g(i) = \exp(-\alpha i)/\exp(-\alpha)$ for $\alpha = 1, 2, 3, 4, 5$.

Fig. 1(c) shows a sigmoid nonlinearity,

$$g(i) = \frac{\tanh(\alpha i)}{\tanh \alpha} \quad (9)$$

for $\alpha = 1, 2, 3, 4$, and 5. Fig. 1(d) shows an exponential nonlinearity,

$$g(i) = \frac{\exp(-\alpha i)}{\exp(-\alpha)}, \quad (10)$$

for $\alpha = 1, 2, 3, 4$, and 5. In both the case of the hyperbolic tangent and exponential ratios, a higher value of α indicates a stronger nonlinearity. The sigmoid nonlinearity, in particular, portrays the properties of a saturating amplifier.

A. Sigmoid Nonlinearity, Cosine Stimulus and Cosine Perturbation

Fig. 2 shows the prediction of the output to a linear system with a sigmoid input-output characteristic, using a cosine waveform as the input operating point and a cosine perturbation of twice the frequency of the operating-point cosine (second harmonic). Fig. 2(a) shows the input, the perturbation, and Fig. 2(b) shows the output approximation and actual signal, where the perturbation has a peak amplitude of one-third of the large-signal amplitude. It can be seen that the output approximation and the signal are nearly identical.

For this simulation, the amplitude of the cosine is insignificant compared to the amplitude necessary to run the sigmoid into compression. Since this nonlinearity is not driven very hard, it tends to mimic a linear response. Regardless of perturbation size, the error significantly drops

for levels of harmonics greater than 1. Fig. 2(c) shows the percent RMS error as a function of the number of harmonics used in the approximation and perturbation size. From this plot it appears that for all perturbation sizes, the error does not significantly decrease when using more than one harmonic for the approximation.

For a sigmoid with stronger nonlinearity, the affine approximation accuracy declines, and shows more dependence upon perturbation size and the number of harmonics used in the approximation. Fig. 3 shows the corresponding results for a strong sigmoid. Fig. 3(c) shows

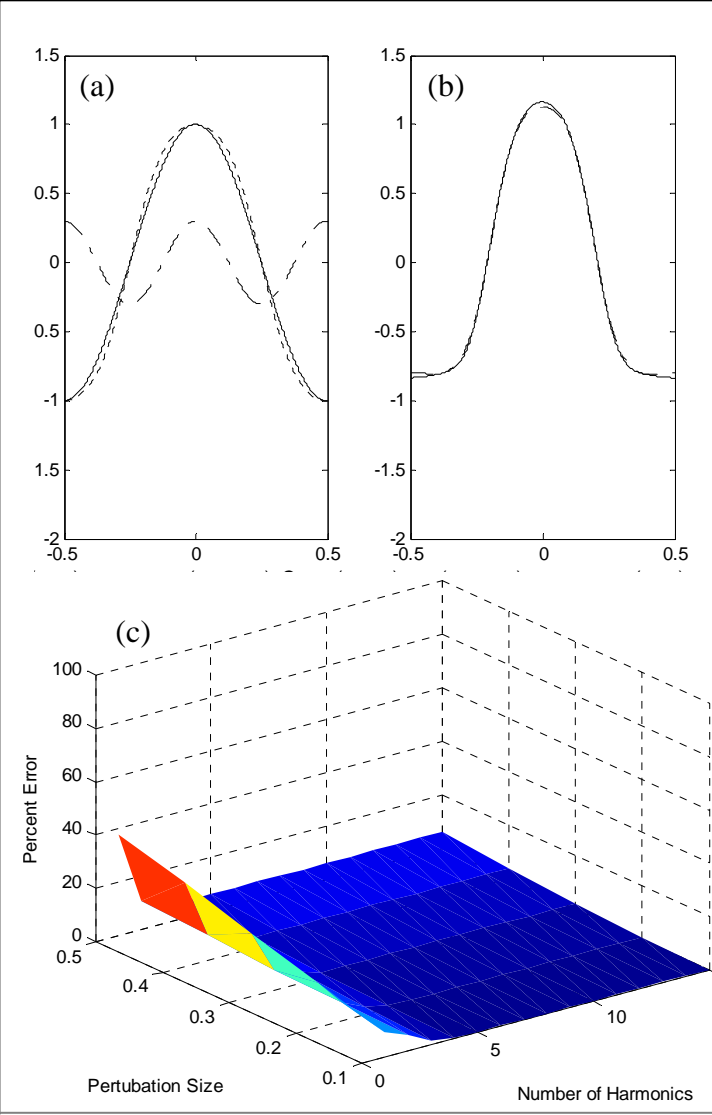


Fig. 2. The solid line in (a) is the sinusoid used as the input to a sigmoid nonlinearity with parameter $\alpha = 1$. The output is the dashed line in (a). The input is perturbed by the dash-dot sinusoid in (a). The true output due to the perturbed input is shown in (b) with a dash-dot line. The TIPP approximation using 15 harmonics, nearly graphically indistinguishable, is also shown in (b) with a solid line. The percent error is shown in (c) as a function of perturbation size and number of harmonics used in the TIPP approximation. The perturbation in (a) is 30% relative to the operating point.

that there is significant error in the affine approximation for all but small perturbation sizes. For low perturbation sizes, 5 harmonics seems nearly sufficient for accurate prediction of the behavior; this is the number of harmonics used in many nonlinear network analyzer measurements. The fact that the error does not improve for additional harmonics at large perturbation sizes seems an indication that the affine approximation is so far from the true response that additional harmonics actually make the approximation worse. These results show consistency with the assumption that perturbations must be small for accurate affine approximation in strongly nonlinear systems.

B. Full-Wave Rectified Nonlinearity, Cosine Operating Point With Cosine Perturbation

Fig. 4 shows the results for a full-wave rectified nonlinearity with a cosine large-signal and a cosine perturbation. As in the first case, the perturbation shown in Fig. 4(a) and 4(b) has an amplitude that is one-third of the large-signal amplitude. As expected, the error seems to increase with increased perturbation size. A significant error can be seen even for large numbers (15 to 20) of harmonics for larger perturbations. The affine model is only valid for small perturbations.

C. Normalized Exponential Nonlinearity, Cosine Operating Point and Cosine Perturbation

Fig. 5 shows results for a weak normalized exponential nonlinearity, while Fig. 6 shows results for a strongly normalized exponential nonlinearity. In both cases, the time-domain plots show a perturbation with an amplitude that is one-third of the large-signal amplitude. The normalized exponential appears to be a good candidate for the affine model when the nonlinearity is weak. The fact that the error is relatively low for even high perturbations indicates that the system is nearly linear about the operating point. This is, however, shown to not be consistent for increasing nonlinearity strength. The strong normalized exponential nonlinearity has the most dramatic error rates among the tested TIPP operators.

III. CONCLUSIONS

The results of the simple TIPP system simulations show that the affine approximation is useful for many nonlinear systems provided (1) the perturbations remains small (the limit of perturbation size depends on the nonlinearity) and (2) a sufficient number of harmonics is used. The number of required harmonics is dependent on the perturbation used. A square wave, for example, has Fourier coefficients that decay as $1/n$ whereas a continuous triangular wave decays as $1/n^2$. More coefficients are therefore required to characterize the square wave.

The accuracy of the affine approximation as the perturbation size increases is, as expected, system dependent. There are TIPP systems for which the affine approximation is ill-suited.

REFERENCES

1. C. Baylis and R.J. Marks II, "Small Perturbation Harmonic Coupling In Nonlinear Periodicity Preservation Circuit," (in review)
2. J. de Graaf, H. Faust, J. Alatishe, and S. Talapatra, "Generation of Spectrally Confined Transmitted Radar Waveforms," Proceedings of the IEEE Conference on Radar, 2006, pp. 76-83.

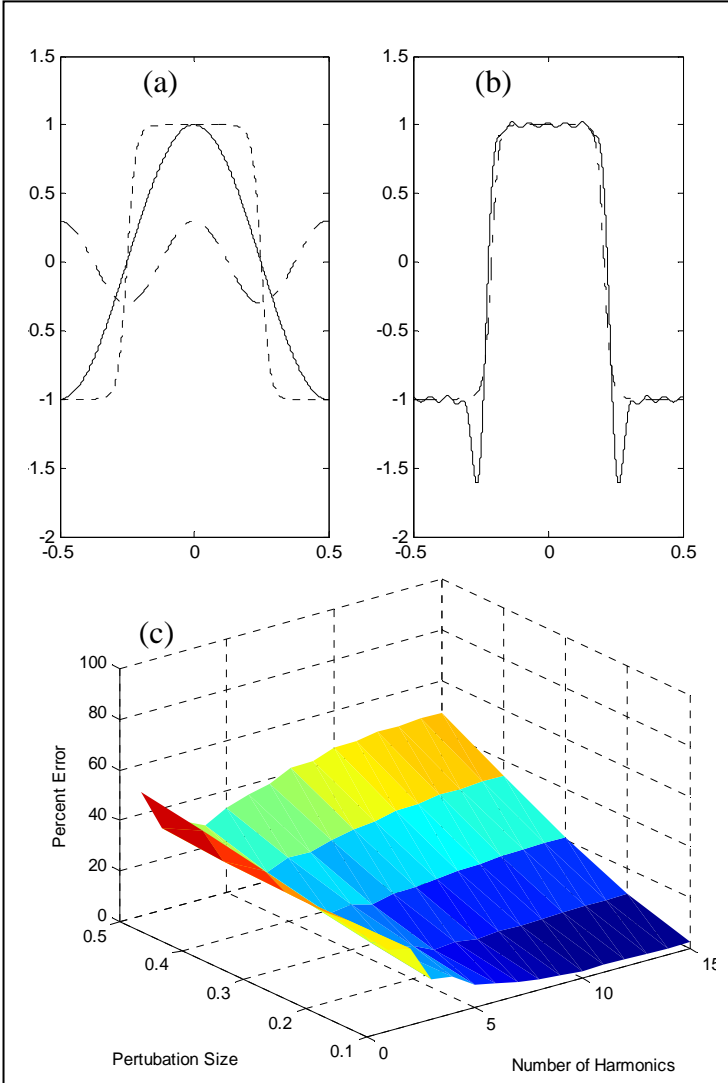


Fig. 3. The solid line in (a) is the sinusoid used as the input to a sigmoid nonlinearity with parameter $\alpha = 5$. This simulation differs from Fig.2 in that the sigmoid is significantly more nonlinear. The output is the dashed line in (a). The input is perturbed by the dash-dot sinusoid in (a). The true output due to the perturbed input is shown in (b) with a dash-dot line. The TIPP approximation using 15 harmonics is also shown in (b) with a solid line. The discrepancy between the approximation and the true output shows the natural limitation imposed by simulating a finite number of harmonics. The percent error is shown in (c) as a function of perturbation size and number of harmonics used in the TIPP approximation. The perturbation in (a) is 30% relative to the operating point.

3. C. Baylis, L. Wang, M. Moldovan, J. Martin, H. Miller, L. Cohen, and J. de Graaf, "Designing Transmitters for Spectral Conformity: Power Amplifier Design Issues and Strategies," Accepted for publication in *IET Radar, Sonar, and Navigation*, June 2011.
4. C. Baylis, L. Wang, M. Moldovan, J. Martin, H. Miller, L. Cohen, and J. de Graaf, "Designing for Spectral Conformity: Issues in Power Amplifier Design," IEEE Waveform Diversity Conference, Niagara Falls, Ontario, Canada, August 2010.
5. Loren Betts, "Vector and Harmonic Amplitude/Phase Corrected Multi-Envelope Stimulus Response Measurements of Nonlinear Devices, *IEEE MTT-S International Microwave Symposium 2008*, pp. 261-264
6. M. Isaksson et al., "A Comparative Analysis of Behavioral Models for RF Power Amplifiers," *IEEE Transactions on Microwave Theory and Techniques*, Vol. 54, No. 1, pp. 348-359, January 2006..
7. J. A. Jargon, K. C. Gupta, and D. C. DeGroot, "Nonlinear large-signal scattering parameters: Theory and application," in 63rd ARFTG Microwave Measurement Conf. Dig., Jun. 2004, pp. 157-174.
8. J. C. Pedro et al., "A Comparative Overview of Microwave and Wireless Power-Amplifier Behavioral Modeling Approaches," *IEEE Transactions on Microwave Theory and Techniques*, Vol.53, No.4, April 2005.
9. J. Wood and D. E. Root, "Fundamentals of Nonlinear Behavioral Modeling for RF and Microwave Design," Chap 3, Artech House, 2005.
10. F. Verbeyst and M. Vanden Bossche, "VIOMAP, the S-parameter equivalent for weakly nonlinear RF and microwave devices," *IEEE Transactions of Microwave Theory & Technology*, vol. 42, no. 12, pp.2531-2535, Dec 1994.
11. M. Myslinski, F. Verbeyst, F.; M. Bossche Vanden, D. Schreurs, "A method to select correct stimuli levels for S-functions behavioral model extraction," *Microwave Symposium Digest (MTT)*, 2010 IEEE MTT-S International , vol., no., pp.1-1, 23-28 May 2010, doi: 10.1109/MWSYM.2010.5518233
12. Guoquan Sun, Yanfeng Xu, Anhui Liang, "The study of nonlinear scattering functions and X-parameters," 2010 International Conference on Microwave and Millimeter Wave Technology (ICMMT), 2010 , pp. 1086 - 1089DOI: 10.1109/ICMMT.2010.5525111.
13. J. Verspecht, M. Vanden Bossche, and F. Verbeyst, "Characterizing components under large signal excitation: Defining sensible 'large signal S-parameters'" in 49th ARFTG Conf. Dig., 1997, pp. 109–117.
14. Jan Verspecht, Dylan F. Williams, Dominique Schreurs, Kate A. Remley, and Michael D. McKinley, "Linearization of Large-Signal Scattering Functions," *IEEE Transactions on Microwave Theory and Techniques*, vol. 53, no. 4, 2005, pp. 1369-1376.
15. Chia-Sung Chiu, Kun-Ming Chen, Guo-Wei Huang, Chih-Hua Hsiao, Kuo-Hsiang Liao, Wen-Lin Chen, Sheng-Chiun Wang, Ming-Yi Chen, Yu-Chi Yang, Kai-Li Wang, Lin-Kun Wu, "Characterization of annular-structure RF LDMOS transistors using polyharmonic distortion model," *IEEE MTT-S International Microwave Symposium Digest*, 2009. MTT '09. pp. 977-980. DOI: 10.1109/MWSYM.2009.5165862.
16. Chia-Sung Chiu, Kun-Ming Chen, Guo-Wei Huang, Shu-Yu Lin, Bo-Yuan Chen, Cheng-Chou Hung, Sheng-Yi Huang, Cheng-Wen Fan, Chih-Yuh Tzeng, Sam Chou, "Power improvement for 65nm nMOSFET with high-tensile CESL and fast nonlinear behavior modeling," 2010 IEEE Radio Frequency Integrated Circuits Symposium (RFIC), pp.589-592. DOI: 10.1109/RFIC.2010.5477258 .
17. D.E. Root, J. Verspecht, D. Sharrit, J. Wood and A. Cognata, "Broad-band polyharmonic distortion (PHD) behavioral models from fast automated simulations and large-signal vectorial network measurements," *IEEE Transactions on Microwave Theory, vol. 53, no. 11, pp. 3656-3664, Nov. 2005.*
18. R.S. Saini, S.Woodington, J. Lees, J. Benedikt, P.J. Tasker, "An intelligence driven active loadpull system," 2010 75th

- Microwave Measurements Conference (ARFTG), pp.1-4. DOI: 10.1109/ARFTG.2010.5496327.
19. J. Verspecht et al., "Multi-port, and Dynamic Memory Enhancements to PHD Nonlinear Behavioral Models from Large-signal Measurements and Simulations", *Conference Record of the*

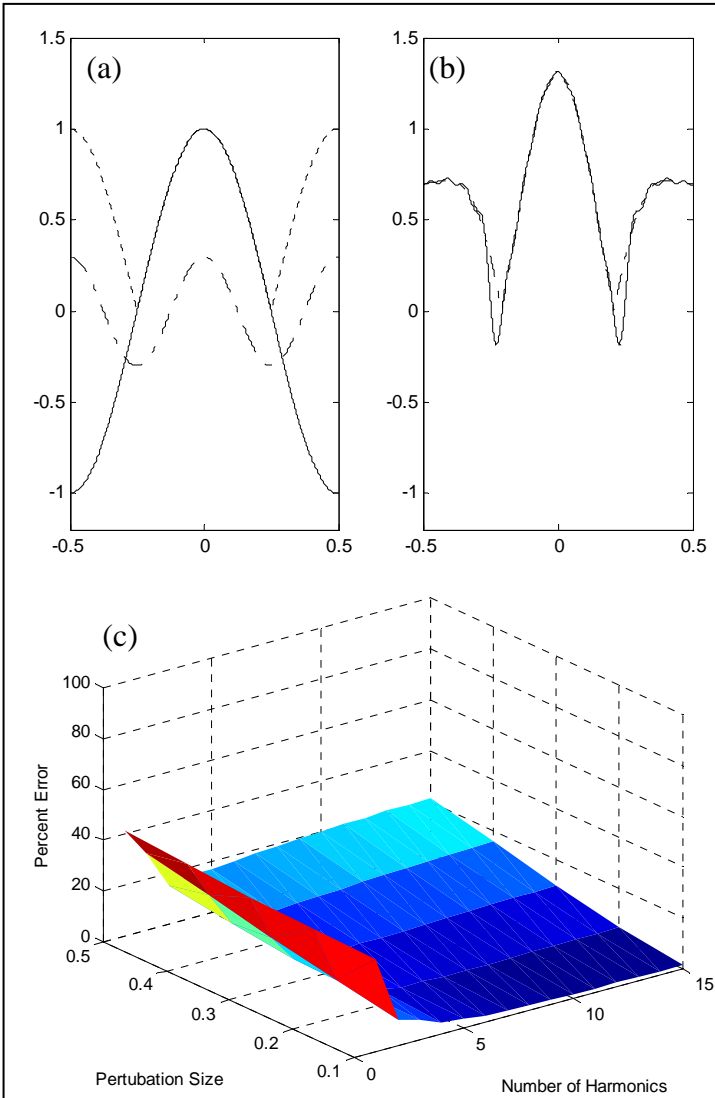


Fig. 4. The solid line in (a) is the sinusoid used as the input to a full-wave rectified nonlinearity. The output is the dashed line in (a). The input is perturbed by the dash-dot sinusoid in (a). The true output due to the perturbed input is shown in (b) with a dash-dot line. The TIPP approximation using 15 harmonics is also shown in (b) with a solid line. Similar results are seen to that in Fig.3, where the approximation is limited by the number of harmonics simulated. The percent error is shown in (c) as a function of perturbation size and number of harmonics used in the TIPP approximation. The perturbation in (a) is 30% relative to the operating point.

- IEEE Microwave Theory and Techniques Symposium 2007*, pp.969-972, USA, June 2007.
20. D.T. Bespalko, S. Boumaiza, "X-parameter measurement challenges for unmatched device characterization," 2010 75th Microwave Measurements Conference (ARFTG), pp.1-4. DOI: 10.1109/ARFTG.2010.5496317

21. D. Gunyan, J. Horn, Jianjun Xu; D.E. Root, "Nonlinear validation of arbitrary load X-parameter and measurement-based device models," 2009 73rd Microwave Measurement Conference, (ARFTG), pp. 1-4. DOI: 10.1109/ARFTG.2009.5278063.
22. J.M.Horn, J. Verspecht, D. Gunyan, L. Betts, D.E. Root, J. Eriksson, "X-Parameter Measurement and Simulation of a GSM Handset Amplifier," 2008 European Microwave Integrated Circuit Conference, EuMIC 2008. pp.135-138. DOI: 10.1109/EMICC.2008.477224
23. Horn, L.Betts, C. Gillease, J. Verspecht, D.Gunyan,D.E. Root, "Measurement-based large-signal simulation of active components from automated nonlinear vector network analyzer data via X-parameters," IEEE International Conference on Microwaves, Communications, Antennas and Electronic Systems, 2008. COMCAS 2008. pp. 1-6. DOI: 10.1109/COMCAS.2008.4562819.
24. J. Randa, "Uncertainty analysis for noise-parameter measurements," Conference on Precision Electromagnetic Measurements Digest, 2008. pp. 498-499. DOI: 10.1109/CPEM.2008.4574871.
25. D.E. Root, J. Xu, J.Horn, M. Iwamoto, G. Simpson, "Device modeling with NVAs and X-parameters," 2010 Workshop on Integrated Nonlinear Microwave and Millimeter-Wave Circuits (INMMIC), pp. 12-15. DOI: 10.1109/INMMIC.2010.5480151.
26. G. Simpson, J. Horn, D. Gunyan, D.E. Root, "Load-pull + NVNA = enhanced X-parameters for PA designs with high mismatch and technology-independent large-signal device models," 72nd ARFTG Microwave Measurement Symposium, 2008, pp. 88 - 91. DOI: 10.1109/ARFTG.2008.4804301.
27. G. Simpson, "High power load pull with X-parameters - a new paradigm for modeling and design," Wireless and Microwave Technology Conference" (WAMICON), 2010 IEEE 11th Annual 2010, pp. 1 - 4 doi: 10.1109/WAMICON.2010.5461843
28. M.S. Taci, I. Doseyen, "Determining the harmonic components of nonlinear impedance loads in terms of resistances and reactances by using a current harmonic method," 9th Mediterranean Electrotechnical Conference, 1998. MELECON 98., Volume: 2, pp. 1000-1003. DOI: 10.1109/MELCON.1998.699379.
29. Jan Verspecht, Jason Horn, Loren Betts, Daniel Gunyan, Roger Pollard, Chad Gillease, David E. Root, "Extension of X-parameters to Include Long-Term Dynamic Memory Effects," Proceedings of the 2009 IEEE International Microwave Symposium - Boston, USA.
30. J. Wood, G. Collins, "Investigation of X-parameters measurements on a 100 W Doherty power amplifier," 75th Microwave Measurements Conference (ARFTG), 2010, pp. 1-7. DOI: 10.1109/ARFTG.2010.5496319.
31. Martin Schetzen, *The Volterra and Wiener Theories of Nonlinear Systems*, Revised edition, Krieger Publishing Company (2006).
32. John B. Thomas, *Introduction to Statistical Communication Theory*, John Wiley & Sons, (1969).
33. C. Baylis, R.J. Marks II, J. Martin, H. Miller, and M. Moldovan, "Going Nonlinear," *IEEE Microwave Magazine*, Vol. 12, No. 2, April 2011, pp. 55-64.

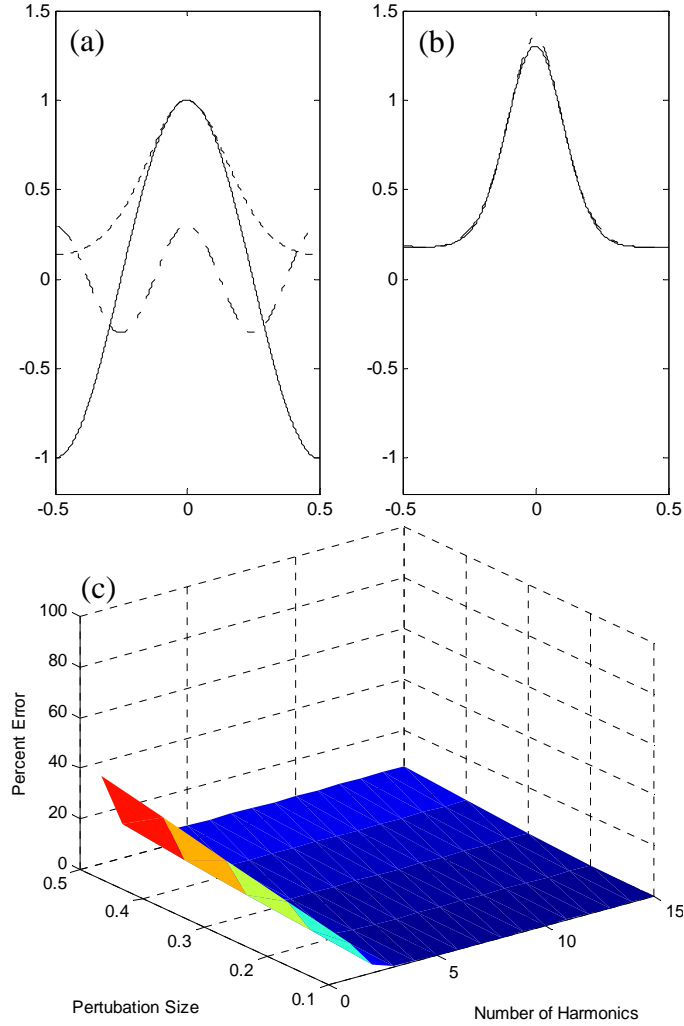


Fig. 5. The solid line in (a) is the sinusoid used as the input to a exponential nonlinearity with parameter $\alpha = 1$. The output is the dashed line in (a). The input is perturbed by the dash-dot sinusoid in (a). The true output due to the perturbed input is shown in (b) with a dash-dot line. The TIPP approximation using 15 harmonics is also shown in (b) with a solid line. The percent error is shown in (c) as a function of perturbation size and number of harmonics used in the TIPP approximation. The perturbation in (a) is 30% relative to the operating point.

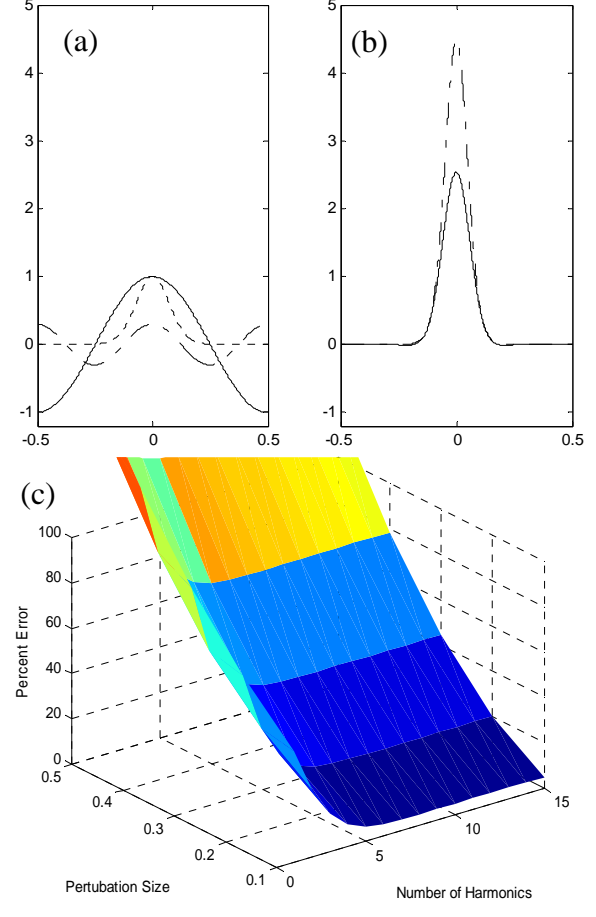


Fig. 6. The solid line in (a) is the sinusoid used as the input to a exponential nonlinearity with parameter $\alpha = 5$. The output is the dashed line in (a). The input is perturbed by the dash-dot sinusoid in (a). The true output due to the perturbed input is shown in (b) with a dash-dot line. The TIPP approximation using 15 harmonics is also shown in (b) with a solid line. These results verify the limitation of TIPP approximation for points of strong nonlinearity, which would require a larger number of harmonics. The percent error is shown in (c) as a function of perturbation size and number of harmonics used in the TIPP approximation. The perturbation in (a) is 30% relative to the operating point.